Applied Energy 238 (2019) 985–995

Contents lists available at ScienceDirect

Applied Energy

journal homepage: www.elsevier.com/locate/apenergy

Fuel consumption and emission characteristics in asymmetric twin-scroll turbocharged diesel engine with two exhaust gas recirculation circuits

Dengting Zhu, Xinqian Zheng*

Turbomachinery Laboratory, State Key Laboratory of Automotive Safety and Energy, Tsinghua University, Beijing 100084, China

HIGHLIGHTS

- A new asymmetric twin-scroll turbocharged engine with two EGR circuits is first presented.
- Experiment and simulation are combined on the diesel engine with asymmetric turbocharger.
- Effect laws of turbine critical parameters and EGR valves control strategy are explored.
- The new system has the maximum EGR rate and fuel economy improvements of 8.59% and 1.98%.

ARTICLE INFO

Keywords:
Asymmetric twin-scroll turbine
Two exhaust gas recirculation circuits
Diesel engine
Emission
Fuel consumption

ABSTRACT

This paper is the first known presentation of an asymmetric twin-scroll turbocharged engine with two exhaust gas recirculation circuits for emission and energy improvements. The traditional asymmetric twin-scroll turbocharged engine has one exhaust gas recirculation circuit, which is simple in structure and can improve the trade-off between low fuel consumption and nitrogen oxide emissions. However, at the high-speed range, the turbine's larger scroll has an exhaust pressure that is higher than the intake pressure, leading to poor fuel economy. A test bench experiment was performed to validate numerical models of the asymmetric twin-scroll turbocharged engine with one and two exhaust gas recirculation circuits. Based on the models, both the influences of critical turbine parameters (turbine asymmetry, efficiency and throat area) on engine emission and fuel consumption characteristics, and the EGR valves and the wastegate control strategy were studied, and they were different from the asymmetric twin-scroll turbocharged engine with one exhaust gas recirculation circuit. The maximum exhaust gas recirculation rate and fuel economy improvements were approximately 8.59% and 1.98%. The new technology of the asymmetric twin-scroll turbocharged engine with two exhaust gas recirculation circuits described in this report has the potential to provide substantial gains in engine emission and energy.

1. Introduction

At present, energy conservation and emission reduction are essential with greater energy shortages and environmental problems being. During the last two decades, internal combustion engines have faced increasing challenges to meet strict emissions legislation [1]. Fossil fuel combustion is the most significant cause of climate change, accounting for 57% of the total greenhouse gas production, mainly caused by industrial and transport emissions [2]. Since the United States first established the Corporate Average Fuel Economy standards in the 1970s, the standards for improving fuel economy have been spread worldwide [3]. Moreover, from the introduction of Euro 1 emission standards in 1993 to the recent implementation of Euro 6, NO_x has been dropped by almost 95 percent, a challenging target for internal combustion engine manufacturers [4]. Tighter laws have prompted engine makers to use exhaust gas recirculation (EGR) and turbocharger technology increasingly.

EGR is recognized as an in-cylinder approach to reducing emissions, especially in modern direct-injection (DI) diesel engines [5]. Over the years, applied to diesel engine EGR rate increased with more strict NO_x emissions targets, because with the increase of EGR rate, in-cylinder peak pressure is reduced, and the fuel combustion heat release is delayed [6]. Almeida et al. [7] established a useful multi-dimensional computational model in demonstrating that the lifted flame concept and high EGR rate was able to meet Euro 6 performance and emissions targets for a 3.2 L engine. Zamboni et al. [8] presented the integrated control of high/low-pressure EGR systems and variable nozzle turbine opening degree, and achieved the reduction of NO_x emissions above

* Corresponding author.
E-mail address: zhengxq@tsinghua.edu.cn (X. Zheng).

https://doi.org/10.1016/j.apenergy.2019.01.188
Received 26 August 2018; Received in revised form 19 December 2018; Accepted 21 January 2019

Nomenclature

φ	turbine throat area
rpm	revolutions per minute
rps	revolutions per second

Subscripts

1	small scroll inlet
2	large scroll inlet

Abbreviation

ASY	turbine scroll asymmetry
ATST	asymmetric twin-scroll turbine
ATSTE-1EGR	asymmetric twin-scroll turbocharged engine with one EGR circuit
ATSTE-2EGR	asymmetric twin-scroll turbocharged engine with two EGR circuits
BSFC	brake specific fuel consumption
C	compressor
DI	direct injection
DL	dual loop
EGR	exhaust gas recirculation
FGT	fixed geometry turbine
HP	high pressure
LP	low pressure
NO_x	nitrogen oxides
OPD	opening degree
PMEP	pumping mean effective pressure
DES	dimensionless engine speed
T	turbine
VGT	variable geometry turbine
WG	wastegate

50% compared to Euro 5 levels. Li et al. [9] experimentally and theoretically investigated the effects of EGR on the mixing performance, combustion, thermal efficiency and NO_x emission of a 6-cylinder natural gas engine. Wei et al. [10] concluded that the combination of EGR technology with other advanced technologies can optimize fuel economy and achieve stricter future emission laws. Nowadays, many turbocharging techniques, including variable geometry turbine (VGT), two-stage turbocharging, symmetric and asymmetric twin-scroll turbines, are widely combined with EGR in automobile diesel engines.

VGT technology is applied to boost pressure and decrease turbocharging turbo lag, and Saidur et al. [11] reviewed that VGT produced different boost pressures for meeting engine requirements by changing the effective aspect ratio. An engine with a VGT has small movable blades which optimize the exhaust flow, to guide incoming exhaust through turbine blades. Hatami et al. [12] carried out the optimization design of VGT blade geometry by applying the central composite sketch based on the experimental design, which exhibited an efficiency of 76.31%. Mao et al. [13] had an experimental study with a heavy-duty commercial diesel engine to investigate the coupling between dual loop EGR and VGT, and the results demonstrated that VGT and high pressure (HP) EGR both significantly influenced turbocharger efficiency. The VGT blade position can set the EGR rate, and therefore, the combined control of EGR and VGT can optimize fuel economy by minimizing pumping losses. However, a very sophisticated control system is required to achieve a better match with the engine. Generally, the cost of a typical engine system with VGT is from 270% to 300% the cost of the same size system without VGT [14].

Two-stage turbocharging is also a well-accepted and effective technology to further recovery waste energy from engine exhaust and reduce fuel consumption [15]. In this system, HP turbine is closer to the exhaust valve, and smaller than LP turbine to implement quick response when the engine starts, and meanwhile, the larger LP turbine boosts for more power output [16]. It is challenging to achieve the current goal of single-stage turbocharging for high EGR rates because of limited turbocharger efficiencies [17]. Nevertheless, one of the unique challenges is more weight, bigger size, more required actuators. It is challenging to match the LP with HP stages, as well as the two-stage turbocharger with the engine [18]. The larger flow passage volume and more metal surface will deferred reaction caused by the turbocharger to warm up from the cold start [19].

The most commonly used configuration of a dual-inlet turbine is a twin-scroll turbine, with a volute casing separated by a meridian, and a separate distributor around the entire circumference of the shell. The twin-scroll turbine was first proposed in 1954 [20] for improving the potential of a turbine operating with a pulsating flow. Because of its cheap and simple design, symmetrical twin-scroll turbines have traditionally been widely used in multi-cylinder engines. This design goes beyond the traditional turbocharger design, which typically only accounts for steady-flow performance and enables improvement of the turbocharger design to achieve enhanced pulsed-flow turbine performance [21]. Rajoo et al. [22] addressed unsteady turbine performance under the combination of twin-entry and variable geometry configurations. Chiong et al. [23] proposed a modified one-dimensional pulse flow model for a turbocharger turbine with a double-vortex turbine. The results suggested that the twin-scroll turbine could not work at full airflow capacity. The symmetric twin-scroll turbine is usually adopted for EGR, and both scrolls are contributed to driving EGR [24].

Currently, twin-scroll turbines are not limited to improving engine power. The severe restriction of emission increasing prompts a manufacturer to develop an asymmetric twin-scroll turbine (ATST). The ATST first emerged in the last century and was used by Daimler-Benz to keep overall fuel consumption increases as low as possible. The small scroll is fed by the exhaust of three cylinders via a split manifold that operates at higher pressure than the exhaust manifold that supplies the larger scroll. Different exhaust pressures are created in the two exhaust branches by the various flow paths in each of the twin scrolls.

In 2008, Müller et al. [25] presented that exhaust gas turbocharger with ATSTs are an essential component of Mercedes-Benz truck engines that use EGR to fulfill the limits for NOx-emissions, and concluded that the ATST allows EGR-transport with little pumping work. Fredriksson et al. [26] developed a mean-line mainline model for a radial inflow turbine with twin-scroll scroll and different total pressures, and total temperatures might be specified at each entry, resulting in a good accuracy of prediction with a realistic set of modeling coefficients. In the same year, Krüger et al. [27] introduced the 10.7 L OM 470 with an ATST which is destined for applications worldwide. After that, Daimler has launched the ATSTs for all its new diesel engines that are to meet the Euro 6 emission levels [28,29]. The heavy-duty diesel engines equipped with ATSTs include the 14.8 L OM472, 12.8 L OM471, 15.6 L OM473 [30]. In asymmetric twin-scroll turbocharged engine modeling, Hand et al. [31] developed techniques which were extended to account for this class of turbines, and a control-oriented, mean value model. In the study of Brinkert et al. [32], the analyzed measurements showed that the interaction of the two turbine scrolls was of great relevance, especially if the turbine scrolls were asymmetric and their response was not reversely identical. Based on these results, Zhu et al. [33] investigated the critical parameters effect laws of the ATST on engine performances and quantitatively analyzed its potential compared with symmetric twin-scroll turbines. Then, they presented a new asymmetric twin-scroll turbine with two wastegates which could achieve the

maximum fuel economy improvement of 2.91% [34].

Typically, the asymmetric twin-scroll turbocharged engine has one EGR circuit linked with the small volute to drive the EGR. However, when the engine operates at the high-speed range, the large scroll exhaust pressure becomes higher than that of the intake, which increases the fuel consumption because of more pumping work.

A new asymmetric twin-scroll turbocharged engine is presented for the first time with two EGR circuits, rather than one EGR circuit. Compared with VGT, two-stage turbocharging, symmetric twin-scroll turbine and asymmetric twin-scroll turbocharged engine with one EGR circuit (ATSTE-1EGR), the asymmetric twin-scroll turbocharged engine with two exhaust gas recirculation circuits (ATSTE-2EGR) is not very complicated and has significant advantages in engine emissions and fuel economy. In this study, both issues that the engine emission and fuel consumption characteristics of ATSTE-2EGR and the EGR valves and the wastegate (WG) control strategy are investigated. Meanwhile, the potential engine performance improvements are evaluated. There are four main parts in this paper. First, an experiment with an asymmetric twin-scroll turbine is performed, and the numerical models are validated. Second, the charge air condition of the ATSTE-1EGR is explored. Third, both the influences of critical turbine parameters (turbine asymmetry, efficiency, and throat area) on engine emission and fuel consumption characteristics, and the EGR valves and the WG control strategy are studied. Lastly, the emissions and fuel economy advantages of an ATSTE-2EGR are evaluated in comparison to an ATSTE-1EGR.

2. Experimental and simulation methods

Normally, the asymmetric twin-scroll turbocharging system provides more energy recovery and less NO_x to internal combustion engines. Fig. 1 presents a schematic diagram of a 6-cylinder diesel engine with an ATST and EGR system. Commonly, the six cylinders are divided into two groups equally, which are respectively linked with the two turbine volutes. The small volute develops a high exhaust pressure, p_1, that is sufficient to drive EGR, and the large volute back-pressure, p_2, is lower to offer a good air exchange. In the design concept, the negative pressure difference between engine intake and turbine inlet is generated in only a small branch. Thus, while some cylinders are served with a high exhaust gas back-pressure, others are operated with a fuel-saving low exhaust gas back-pressure. The turbine asymmetry (ASY), which is commonly defined by the ratio of the throat areas of the two volutes (Eq. (1)), is intended to influence the EGR rate and associated raw NO_x emissions on one hand and the air-fuel ratio and the achievement of optimal gas exchange over the entire operating range on the other side [35].

$$ASY = \frac{\varphi_1}{\varphi_2} \times 100\% \tag{1}$$

where $\varphi_1$is the small volute throat area, and $\varphi_2$is the large volute throat area. ASY is a crucial parameter which can characterize the two volutes differences.

This experiment was conducted on a water-cooled, 12.55 L, 4-valve, 6-cylinder diesel engine. It had an asymmetric twin-scroll turbocharging system (ASY = 53%) and an intercooled EGR system. The engine maximum torque and the rated power are 2380 N m (1100–1400 rpm) and 351 kW (1900 rpm), respectively. The technical specifications of the test engine are listed in Table 1. According to Fig. 1, the whole experimental engine system was established on a dynamometer test bench. The primary testing tools are given in Table 2. The test engine worked at the operation of full load and various speeds.

Fig. 2 shows the engine simulation model that is established and validated by the engine cycle simulation software (GT-SUITE v7.3.0). The test bench combustion rate is used for the engine combustion model. In the experiment, an AVL641 combustion analyzer was adopted to measure and obtain the heat release rate ($\frac{dQ}{dt}$) and the quantity of combusted fuel per unit time ($\frac{dm}{dt}$) as shown in Eq. (2).

$$\frac{dm}{dt} = \frac{\frac{dQ}{dt}}{Hum} \tag{2}$$

where Hum is the calorific value of the mixture. “Combustion rate” is defined as the quantity of fuel combusted per unit time ($\frac{dm}{dt}$) expressed as a percentage of the total injection mass per cycle (mt).

$$Combustion\ rate = \frac{\frac{dm}{dt}}{mt} \times 100\% \tag{3}$$

The experimental combustion data for full load is exhibited in Fig. 3. The dimensionless engine speed (DES) is normalized to the maximum engine speed at the full load (1900 rpm). The empirical WoschniGT is applied to the heat transfer model which indicates that the in-cylinder heat transfer will be calculated by a formula which closely emulates the classical Woschni correlation without swirl [36]. An essential difference lies in the treatment of heat transfer coefficients during the period when the valves are open, where the heat transfer is increased by inflow velocities through the intake valves and also by backflow through the exhaust valves. This heat transfer coefficient calculated by this model will decrease to zero as the engine speed decrease to zero. For all multi-zone combustion models, the convection temperature evaluation is calculated as Eq. (4).

$$Tg = Tb\left(\frac{m_b}{m_t}\right)^n + Tu\left(1 - \left(\frac{m_b}{m_t}\right)^n\right) \tag{4}$$

In which Tg is the effective gas temperature, Tb is the burned zone temperature, Tu is the unburned zone temperature, mb is the burned mass, mt is the total mass, and n is the weighting exponent which is calculated from linear to quadratic and the weighting exponent as follows:

$$n = 1 + \left(\frac{m_b}{m_t}\right)^2 \tag{5}$$

The EGR circuit is linked with the small scroll and the EGR valve, which is a check valve, controls the EGR flow. The compressor and turbine (ASY = 53%) maps in Fig. 4 are from turbocharger experiments on the dynamometer test bench. The experimental engine operating conditions are presented in Table 3, and these conditions were entirely adopted in the numerical models. Fig. 5 illustrates the performance validation of the intake and exhaust system including the intake mass flow rate, turbine’s large scroll pressure, and small scroll pressure. The ordinates are dimensionless to the experimental value at the engine speed of 800 rpm. The maximum relative error is within 2.0%. Moreover, the intake temperature and pressure were controlled accurately by the intercooler and the degree of the turbine WG opening, respectively. Meanwhile, the study has compared the experimental and

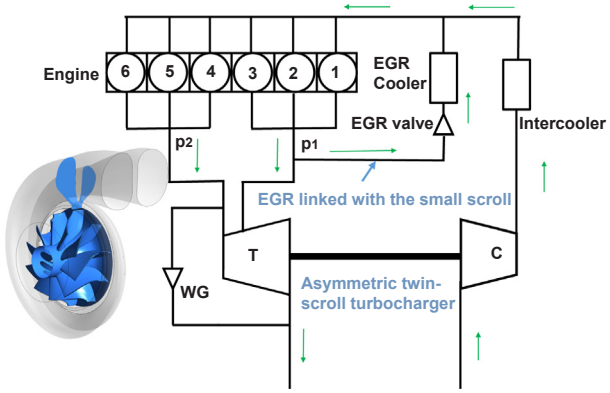

Fig. 1. Schematic diagram of a 6-cylinder diesel engine with an ATST and EGR system.

Table 1
Test engine specifications.

Items	Value and unit
Engine type	Inline 6-cylinder DI diesel
Number of valves per cylinder	4 (2 inlet/2 exhaust)
Bore	129 mm
Stroke	160 mm
Displacement	12.55 L
Compression ratio	18.2:1
Cooling system	Water cooled
Air intake system	Intercooled asymmetric twin-scroll turbocharger (ASY = 53%)
EGR system	Intercooled EGR
Rated power	351 kW (1900 rpm)
Maximum torque	2380 N m (1000–1400 rpm)

simulation results for the model validation. Fig. 6 consists of the contrasts of the engine dimensionless torque, power, brake specific fuel consumption (BSFC), and EGR rate. There is only a low deviation between the experiment and emulation results. For this research, the differences are considered to be acceptable.

3. Charge air gas exchange conditions of ATSTE-1EGR

As previously described for ATSTE-1EGR, the EGR is linked with the small scroll which has a higher exhaust pressure, and the large scroll reduces the average exhaust back-pressure for good fuel economy. However, the back-pressures of the two scrolls and the intake manifold are ever-changing for different engine operations. This section mainly analyzes the gas exchange conditions in the ATSTE-1EGR under different ASY and engine speeds.

Using the model shown in Figs. 2, 7(a) and (b) illustrate the pressure in the turbine small and large scrolls, respectively, relative to the charge air pressure with the EGR valve held fully open while altering the turbine ASY. In Fig. 7(a), the small scroll pressure increases relative to the intake manifold pressure with increasing engine speed. This finding is observed because the exhaust gas pressure increased while the boost-pressure was limited by the maximum torque point for the adjusted degree of the WG opening. The results turn out the pressure in the small scroll is always higher than that of the charge air, which can drive recirculation. Simultaneously, the relative pressure decreased with ASY since a higher ASY means a greater throat area of the small scroll, which drops the exhaust pressure in the cylinders [37]. In contrast, the large scroll usually has a lower exhaust pressure than the intake manifold for a lower pumping loss. With increasing ASY, the large scroll has a smaller throat area, and therefore the pressure difference increases. However, as the engine speeds up, the exhaust pressure increases, exceeding the intake pressure as seen in Fig. 7(b). The relative pressure has a maximum value of 15.18% at 70% ASY and 100% DES between the pressures of the large volute and the intake passages. Consequently, the results indicate that at high engine speeds, the pressures in both turbine scrolls are higher than that of the charge air, which leads to poor conditions for gas exchange.

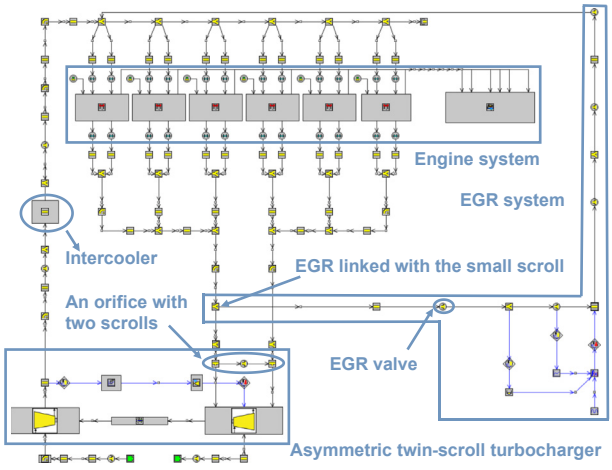

Fig. 2. GT-POWER model of a 6-cylinder diesel engine with an ATST and EGR system.

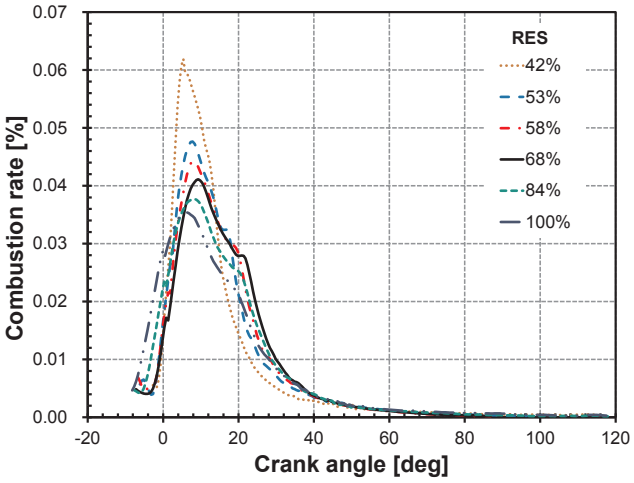

Fig. 3. Experimental combustion rate data of the engine.

To improve the condition of air exchange at the high-speed range, a new ATSTE-2EGR is performed, with an engine system schematic in Fig. 8(a). Based on the simulation model of the ATSTE-1EGR, the model of the ATSTE-2EGR was established as shown in Fig. 8(b). Compared to Fig. 2, the engine system and asymmetric twin-scroll turbocharger were unchanged, and only the structure of the EGR system was different. There were two EGR circuits, one for each exhaust manifold, and the EGR rate was controlled by two EGR valves, with $(\text{EGR valve})_1$ for the small scroll and $(\text{EGR valve})_2$ for the large scroll. Usually, the exhaust gas from the two EGR circuits was first cooled, increasing its density and reducing the temperature for intake, and then sent to the cylinders. At the high-speed range of the engine, the large scroll has higher pressure than the intake, which drives the EGR while also decreasing

Table 2
Test instruments specifications.

Instruments	Types (range and accuracy)
Eddy current dynamometer	C 500 (0–4000 N m and 0–720 kW; ± 10 rpm and ± 1.25 N m)
Fuel consumption measuring instrument	AVL735S (0.1–110 kg/h, 0.12%)
Data acquisition system	PUMA OPEN 1.2
Intake system	Sensyflow P/4000 (± 5mg)
Coolant constant temperature control device	AVL553 (70–120 °C)
Gas emission analyzer	MEXA-7100DEGR
Fuel constant temperature control device	AVL753 (15–80 °C)
Environment simulation system	ACS2400 (298 ± 1 K and 100 ± 1 kPa)

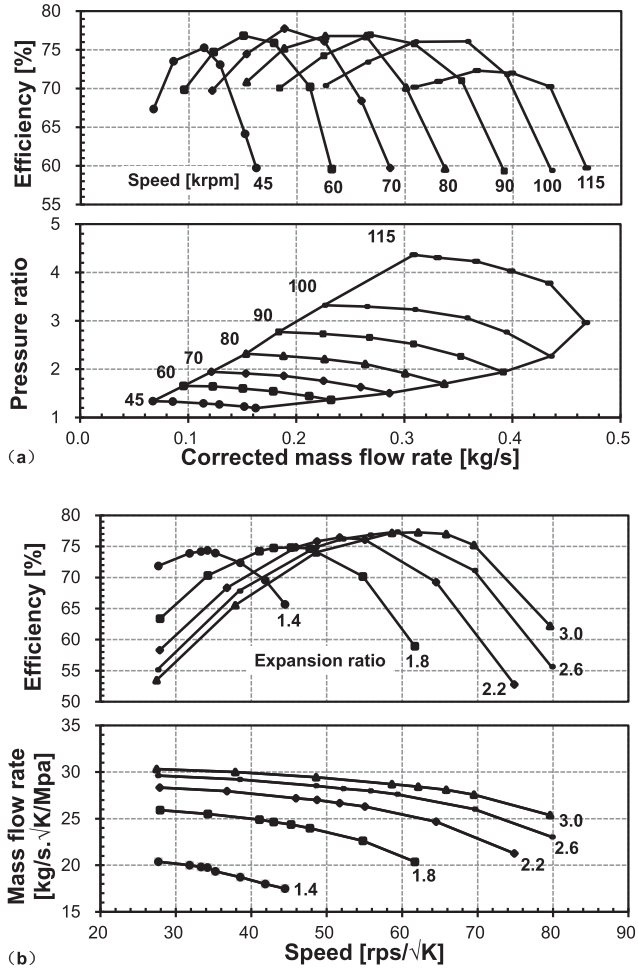

Fig. 4. Turbocharger maps: (a) compressor; (b) asymmetric twin-scroll turbine (ASY = 53%).

Table 3
Experimental engine operating conditions.

Speed (rpm)	Torque (N m)	Power (kW)	Atmospheric pressure (kPa)	Atmospheric temperature (K)	Atmospheric humidity (%)	Fuel mass (kg/h)
800	1818	152	99.34	298.4	39.9	30.92
1000	2385	250	99.31	298.6	40.7	48.72
1100	2385	275	99.33	298.5	40.9	52.76
1200	2386	300	99.33	298.1	40.8	57.68
1300	2385	325	99.33	298.5	40.8	63.00
1400	2385	350	99.30	298.6	40.8	68.85
1600	2096	351	99.34	298.7	39.9	71.07
1900	1761	350	99.37	298.8	38.4	75.52

the average exhaust pressure resulting in better fuel economy.

4. Comparison of ATSTE-2EGR and ATSTE-1EGR

In this part, The ATSTE-2EGR's improvements on engine emissions and fuel economy are investigated compared with the ATSTE-1EGR. It is significant for a better balance between engine emissions and fuel economy to explore the influences of critical parameters (turbine ASY, throat area, and efficiency) and the control strategy of the two EGR valves and one WG. Ref. [33] studied in detail the influences of crucial turbine parameters on ATSTE-1EGR performance including torque, power, BSFC and EGR rate. In this section, a comparison is performed of

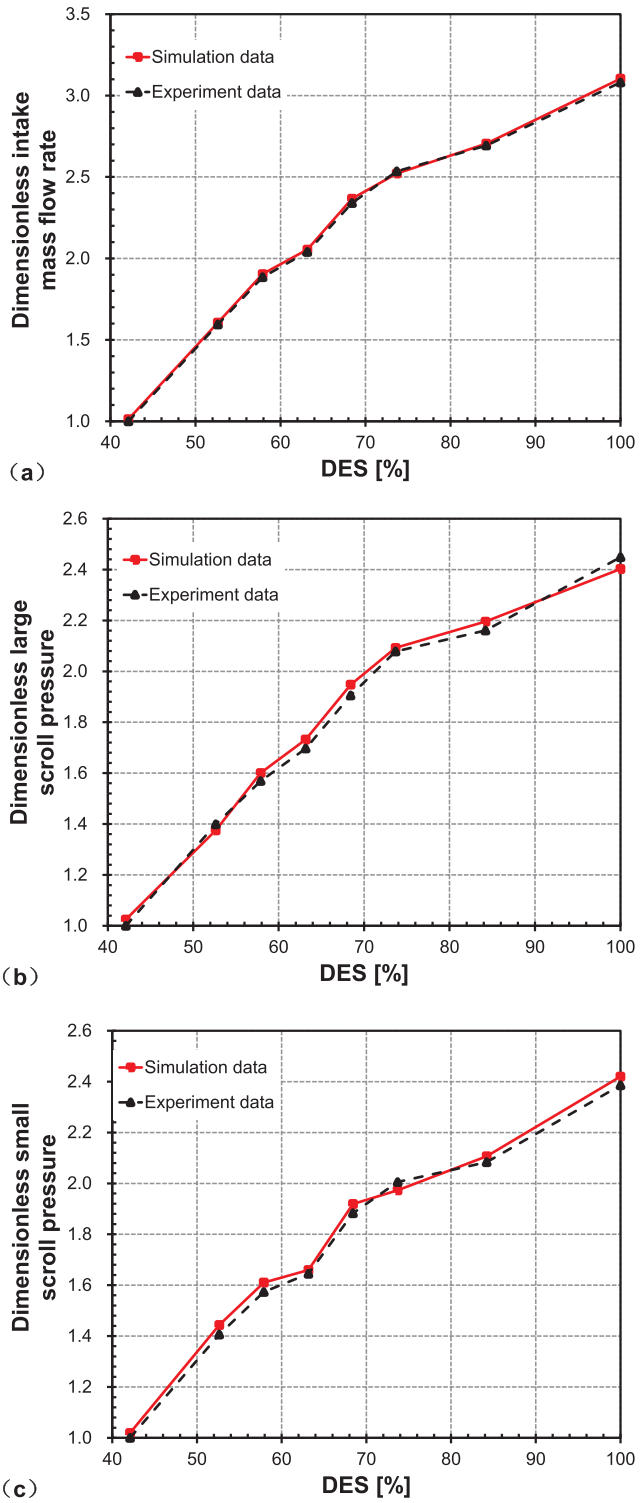

Fig. 5. Performance calibration of the intake and exhaust system: (a) intake mass flow rate, (b) turbine's large scroll pressure, (c) turbine's small scroll pressure (all values are dimensionless due to division by the experimental value at 42% DES).

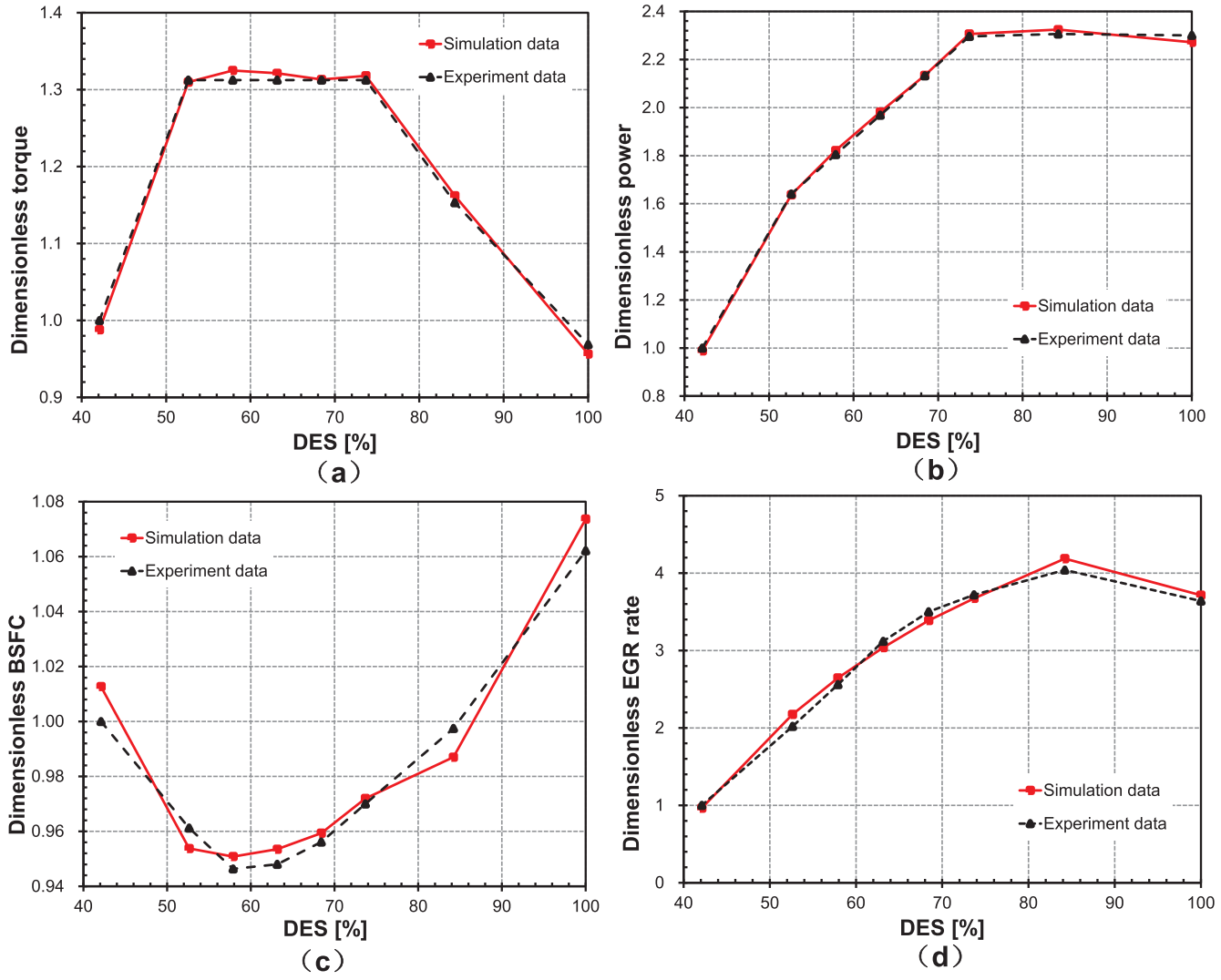

Fig. 6. Performance calibration of the engine system: (a) torque, (b) power, (c) BSFC, and (d) EGR rate (all values are dimensionless due to division by the experimental value at 42% DES).

the different parameters effect laws in the engine cycle simulations of the ATSTE-2EGR and ATSTE-1EGR.

4.1. Influences of turbine key parameters on engine performances

4.1.1. Turbine ASY

ASY is a crucial parameter that characterizes the interrelationship of the two scrolls, and it determines the distribution of exhaust flow for the two turbine volutes. First, based on the models of the ATSTE-2EGR and ATSTE-1EGR, engine cycle simulations were conducted. Keeping the two EGR valves fully open and the boost-pressure the same, both models operated at full engine load while the ASY was changed from 40% to 70%. The differences between ATSTE-2EGR and ATSTE-1EGR as a percentage of ATSTE-1EGR for BSFC and EGR rate at 100% DES were presented in Fig. 9. The results indicated that the ATSTE-2EGR has better emissions and fuel economy. An ASY increase of 10% resulted in the relative EGR rate increasing by approximately 1.28% and BSFC decreasing by 0.56%, with the maximum benefits being 8.59% and 1.98%, respectively. As was also concluded in Section 3, the exhaust pressure in the large scroll was higher than in the intake at high speeds. The pressure differences between the large scroll and the intake can be used to drive the EGR.

In the HP EGR system, Zamboni G et al. [38] have concluded that the pressure gradient of the engine intake and exhaust is the main influencing factor, and both the EGR rate and BSFC decrease with the pressure gradient reducing. To compare the pumping loss, the p-V diagrams of the ATSTE-2EGR and ATSTE-1EGR at 70% ASY and 100% DES were demonstrated in Figs. 10(a) and 1(a), and only the pumping loop diagrams were certified in Figs. 10(b) and 11(b). Figs. 10 and 11 showed the pressures of the Cylinder 1 with the turbine's small scroll and the Cylinder 4 with the turbine's large scroll, respectively. The cylinders of the same cylinder group had the same performance. The cylinders linked with either scroll in ATSTE-2EGR had lower pumping losses compared with the respective cylinders in the ATSTE-1EGR, especially the cylinders with the large scroll (the area enclosed by the closed curve is the pumping work). For the ATSTE-2EGR, both of the EGR valves are entirely open, which means an enlarged turbine throat area leading to lower exhaust pressure. Fig. 12 contained the engine pumping mean effective pressure (PMEP) for 40–80% ASY. The large scroll had a smaller throat area with greater ASY so in the ATSTE-2EGR, the EGR rate was able to increase with a smaller PMEP, but this was not possible in the ATSTE-1EGR. The maximum PMEP difference between the ATSTE-1EGR and the ATSTE-2EGR was 0.37 bar at 70% ASY. Therefore, on the one hand, the EGR from the large scroll offers lower NO_x emissions, and on the other hand, it reduces the pumping loss causing less energy consumption.

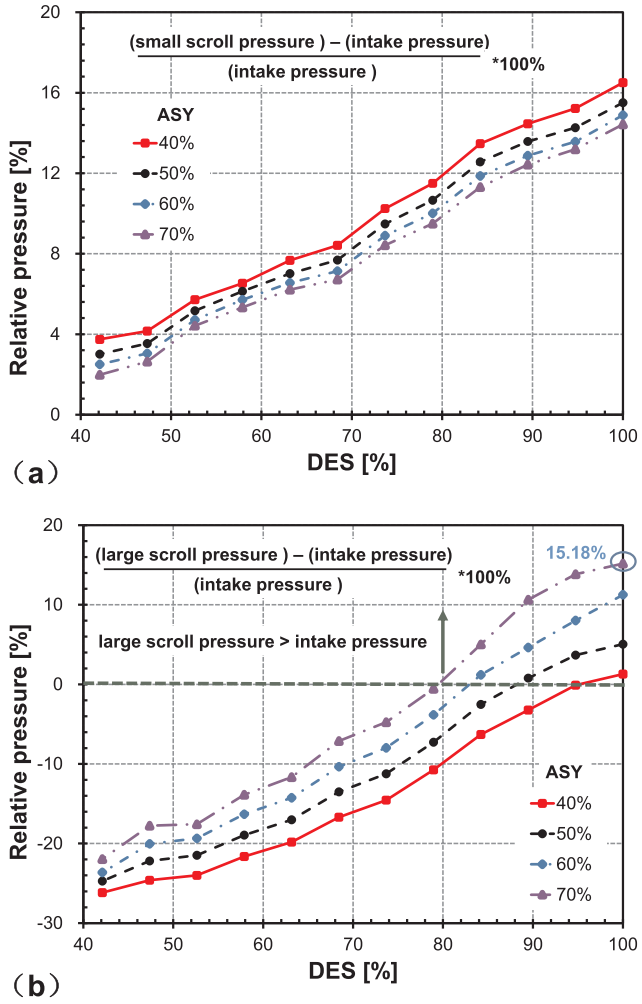

Fig. 7. Simulated pressure relative to the intake manifold for (a) the small scroll; and (b) the large scroll.

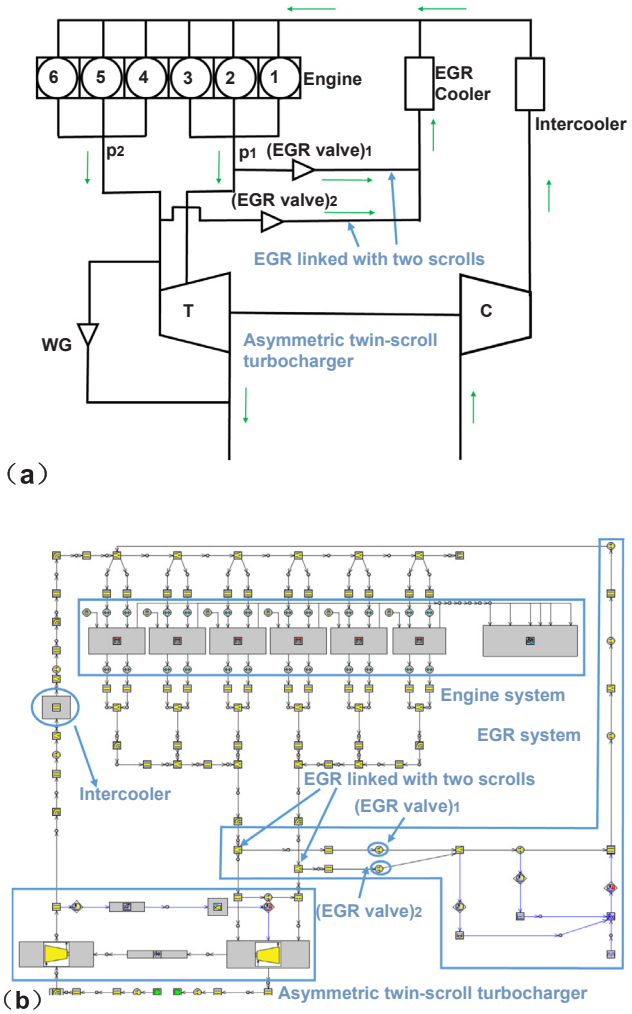

Fig. 8. Asymmetric twin-scroll turbocharged engine with two EGR circuits: (a) the schematic diagram; (b) the simulation model.

4.1.2. *Turbine efficiency*

In considering efficiency characteristics of the asymmetric twin-scroll turbine, it is well-known that the flow on the turbine outlet side achieves a higher level of efficiency than the flow on the bearing casing side [25]. High turbine efficiency is very significant and is always wanted when matched with the engine. In the efficiency tests, both models had the same ASY value of 70% at 100% DES, and only the turbine efficiency was altered. Between the ATSTE-2EGR and the ATSTE-1EGR, the BSFC and EGR rates differences versus changes in efficiency were shown in Fig. 13 with the BSFC and EGR rate differences expressed as a percentage of the value for the ATSTE-1EGR. At different efficiencies, the ATSTE-2EGR showed improvements in both EGR rate and BSFC compared to the ATSTE-1EGR, and the magnitude of the improvements increased with decreasing efficiencies. The maximum EGR rate and BSFC benefits were 10.60% and 1.57%, respectively. For the ATSTE-1EGR, decreasing efficiencies reduced the power of the turbine, and the exhaust back-pressure increased causing worse charge air exchange conditions. Contrarily, for the ATSTE-2EGR, the EGR circuit with the large scroll passage reduced pumping losses. The engine PMEP of ATSTE-2EGR and ATSTE-1EGR was presented in Fig. 14. Increasing efficiency is beneficial for engine performance. The ATSTE-2EGR had higher PMEP than the ATSTE-2EGR resulting for lower pumping losses, and the maximum PMEP difference between the two engine systems was 0.33 bar at the efficiency change of −4%.

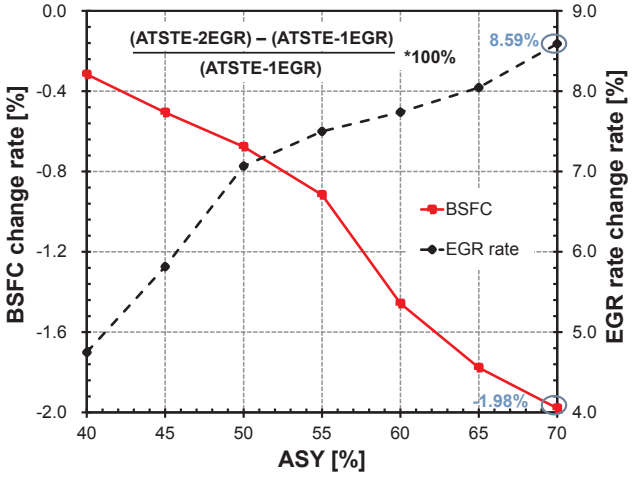

Fig. 9. Difference between ATSTE-2EGR and ATSTE-1EGR as a percentage of ATSTE-1EGR for BSFC and EGR rate versus the ASY range of 40–70%.

4.1.3. *Turbine throat area*

Turbine throat area, which directly influences the turbocharger performance, is a critical design parameter. The effect of changing the throat area on BSFC and EGR rates was shown in Fig. 15, in which BSFC and EGR rate differences between the ATSTE-2EGR and the ATSTE-

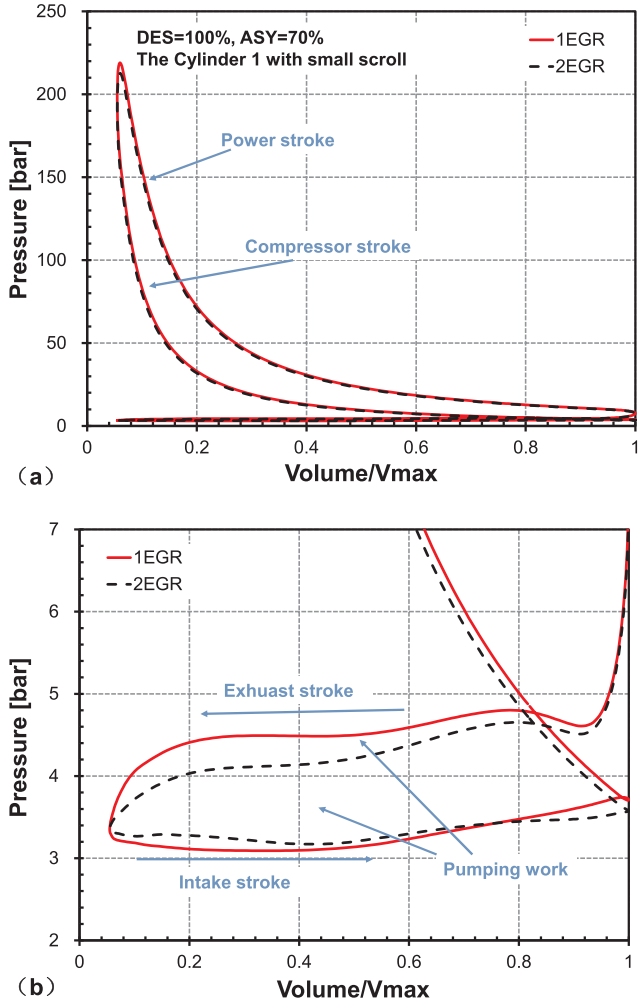

Fig. 10. p-V diagrams for the cylinders connected with the small scroll in the ATSTE-2EGR and ATSTE-1EGR: (a) the complete p-V diagram and (b) the pumping loop portion of the diagram.

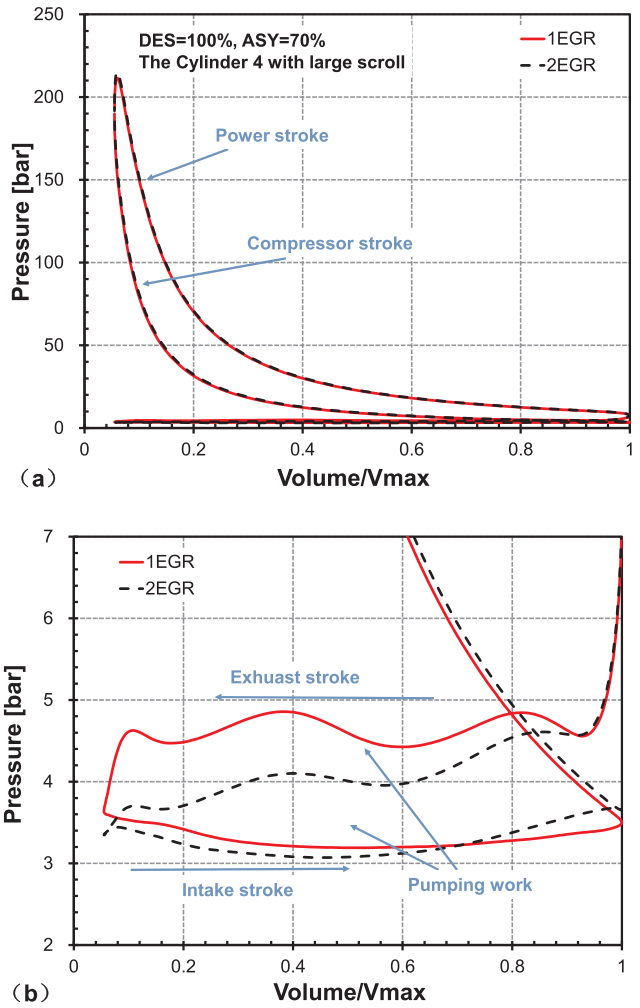

Fig. 11. p-V diagrams for the cylinders connected with the large scroll in the ATSTE-2EGR and ATSTE-1EGR: (a) the complete p-V diagram and (b) the pumping loop portion of the diagram.

1EGR were expressed as a percentage of the values for the ATSTE-1EGR. Similar to the effects seen with changes in turbine efficiency, with changes in the throat area, the ATSTE-2EGR showed improvements in EGR rate and BSFC, and the improvements increased with decreases in the throat area. The maximum EGR rate and BSFC improvements of approximately 11.13% and 1.45% were for a −6% change in the throat area. A larger throat area usually reduces the exhaust gas pressure, and therefore the pressure differential between the large scroll and the intake manifold may weaken the influence of the EGR circuit with the large scroll. The PMEP increased with throat area resulting in lower pumping losses as shown in Fig. 16, and there was a maximum PMEP gain of 0.32 bar due to the increase of the throat area for the ATSTE-2EGR. However, due to engine compartment space limitations, the turbine size should be designed within a proper range.

4.2. EGR valves and WG control strategy

In the existing asymmetric twin-stroll turbocharged engine, the WG with the turbine's large scroll influences the average exhaust back-pressure, and can adjust the boost-pressure to avoid over boosting. Meanwhile, the EGR valve with the small scroll can control the EGR rate, and affect the small scroll back-pressure. Ref. [34] has studied the control strategy of the WG and the EGR valve under different engine operations in the ATSTE-1EGR. For the ATSTE-2EGR, it has one WG with the large scroll and two EGR valves with the two scrolls

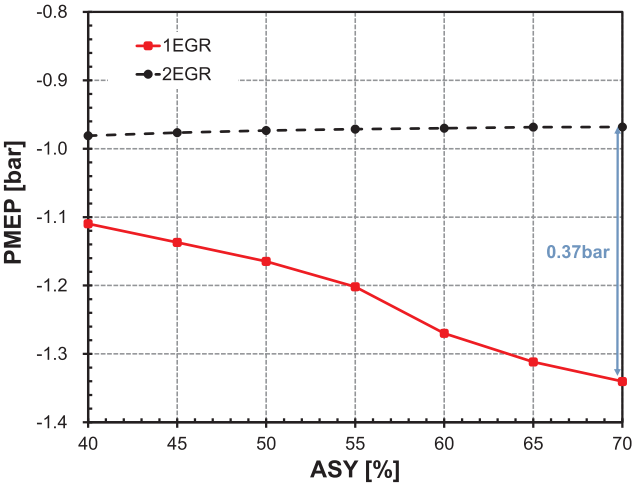

Fig. 12. Engine PMEP in the ATSTE-2EGR and ATSTE-1EGR at 100% DES versus the ASY range of 40–70%.

respectively. The three valves all influence the back-pressures of the two exhaust passages and the engine EGR rate. Therefore, the ATSTE-2EGR has a new control strategy of the WG and EGR valves.

As mentioned above, the two EGR valves are one-way valves, and

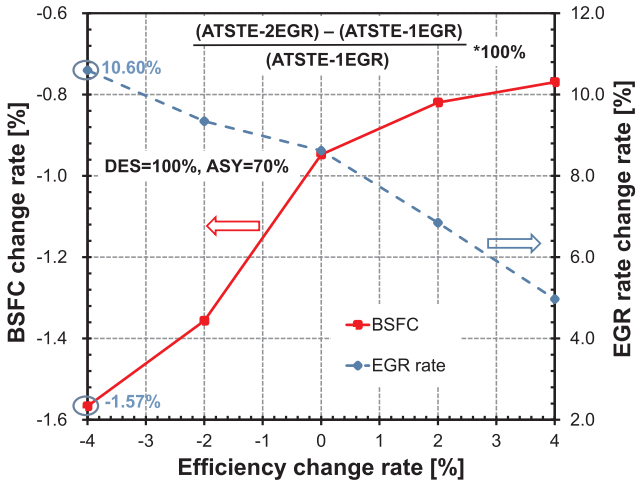

Fig. 13. Difference between ATSTE-2EGR and ATSTE-1EGR as a percentage of ATSTE-1EGR for BSFC and EGR rate versus changes in efficiency.

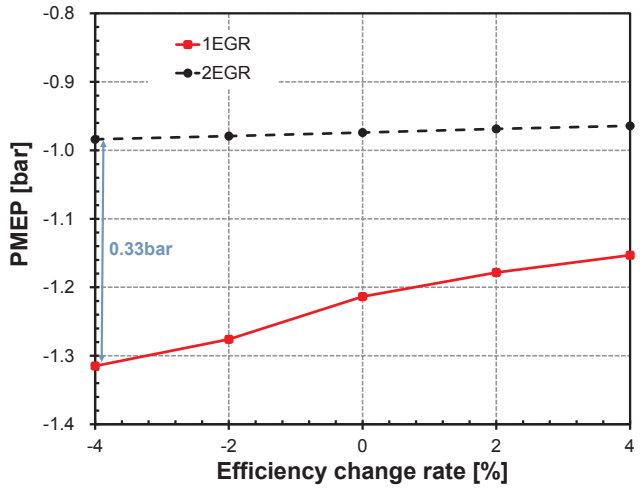

Fig. 14. Engine PMEP in the ATSTE-2EGR and ATSTE-1EGR at 100% DES versus changes in efficiency.

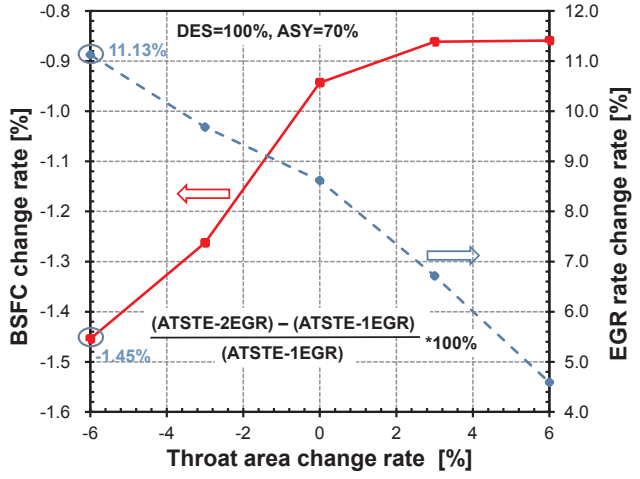

Fig. 15. Difference between ATSTE-2EGR and ATSTE-1EGR as a percentage of ATSTE-1EGR for BSFC and EGR rate versus change in throat areas.

they only allow the gas from the exhaust passages to the intake passage. At different opening degrees (OPD) of the (EGR valve)$_1$ and (EGR valve)$_2$, the WG OPD was taken from Fig. 17(a) and (b). Usually, the WG is fully closed for boosting intake gas within the engine maximum torque point. In Section 3, it's known that the large scroll pressure is lower than the intake pressure at the low and medium speed ranges of the engine, but that's opposite at the high-speed range. Therefore, (EGR valve)$_2$ is completely open beyond about 80% DES and entirely closed within 80% DES in Fig. 17(a). With the (EGR valve)$_1$ OPD decreasing, the EGR flow rate will reduce, and the flow rate into the turbine will increase. Hence, the WG OPD should increase to avoid over-boosting. The engine boost pressure will be in an appropriate range by adjusting the WG. Given a 100% OPD of the (EGR valve)$_1$, Fig. 17(b) showed the control relationship between the WG and the (EGR valve)$_2$ at different engine speeds. At the high-speed range, the (EGR valve)$_2$ opens and influences the flow rate of the large scroll EGR circuit, which increases the total EGR rate and meanwhile reduces the large scroll pressure. Therefore, it will bring EGR rate and BSFC improvements.

To maximize the EGR rate, the EGR valves and the WG should be adjusted at the same time. In the ATSTE-1EGR (Fig. 18(a)), the EGR valve wholly opens and the WG has a applicable for boosting. In the ATSTE-2EGR (Fig. 18(b)), the (EGR valve)$_1$ also has a 100% OPD. The (EGR valve)$_2$ first completely closes when the large scroll pressure is smaller than the intake pressure, and then completely opens when the large scroll pressure is higher. Because of the limited boosting pressure, the intake pressure is the same at the same engine speed in the ATSTE-1EGR and ATSTE-2EGR. Therefore, the WG OPD of the ATSTE-2EGR will be smaller than that of the ATSTE-1EGR. The ATSTE-2EGR has higher EGR rate, so the exhaust gas through the WG should be decreased to ensure the same turbine work.

4.3. EGR rate and BSFC improvements in the ATSTE-2EGR

From the sections above, it is clear that the ATSTE-2EGR has obvious advantages than the ATSTE-1EGR concerning engine performances. The maximum improvements in EGR rate and BSFC in the ATSTE-2EGR as compared to the ATSTE-1EGR were provided in Fig. 19 for different engine speeds with 70% ASY and the same engine power. There was no change in EGR rate differences at lower speeds, but at higher speeds, the differences increased with the engine speed. Meanwhile, at higher speeds, the BSFC differences were inversely related to the engine speed. It was already found in Section 3 that the large scroll exhaust pressure was lower than the intake pressure at low and medium speeds (with less than 80% DES); thus, the (EGR valve)$_2$ was fully closed at these speeds, which resulted in the identical performance of the ATSTE-2EGR and the ATSTE-1EGR. However, at the high-speed range, the (EGR valve)$_2$ is fully open, and the large scroll starts to drive EGR. When the engine speed was above 80% DES, a 10% increase in speed resulted in EGR rate differences increasing by about 4.09%, and BSFC differences decreasing by approximately 0.94%. The EGR rate and BSFC had maximum improvements of 8.59% and 1.98%, respectively, because the ATSTE-2EGR has two EGR circuits, which means the throat area can be increased to provide lower average exhaust pressure and lower pumping losses. Consequently, at the high-speed range of the engine, the ATSTE-2EGR has better emission and energy performances than the ATSTE-1EGR.

5. Conclusions

A new asymmetric twin-scroll turbocharged engine with two EGR circuits is performed to gain NO_x emissions and energy improvements. To describe the engine's potential improvements, this work compared the EGR rate and BSFC performance of an asymmetric twin-scroll turbocharged engine with two EGR circuits, and one EGR circuit, respectively. The effects of changes in critical turbine parameters and the control strategy of the ECR valves and wastegate were investigated. The most significant results are the following:

(1) In the asymmetric twin-scroll turbocharged engine with one EGR

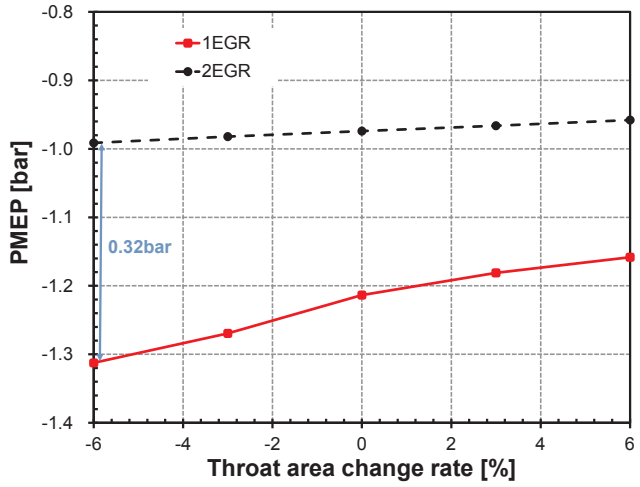

Fig. 16. Engine PMEP in the ATSTE-2EGR and ATSTE-1EGR at 100% DES versus changes in throat area.

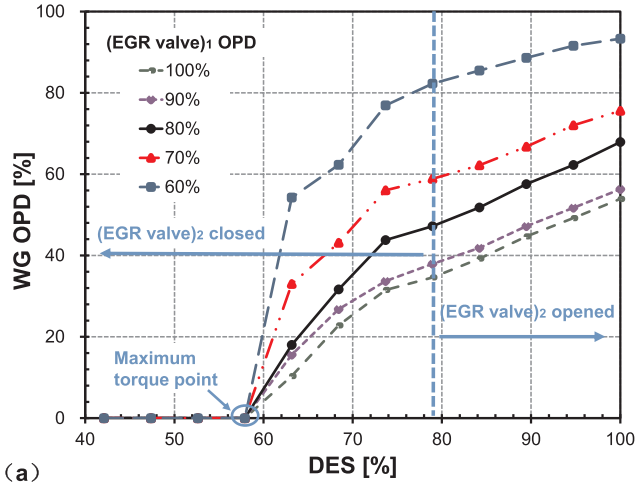

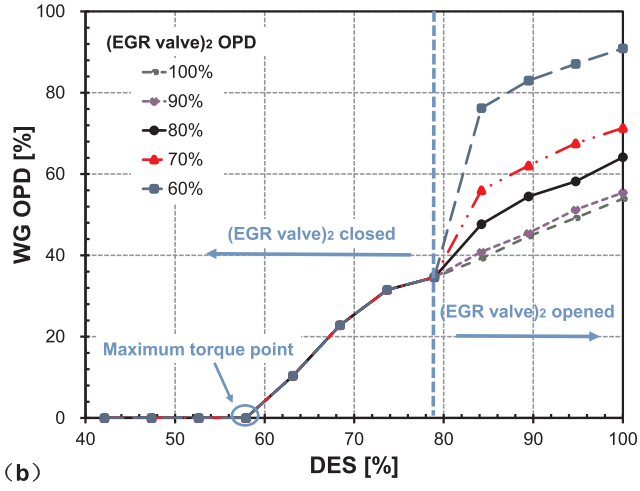

Fig. 17. WG OPD in the ATSTE-2EGR at different (a) $(EGR\ valve)_1$ OPDs, and (b) $(EGR\ valve)_2$ OPDs.

circuit, the back-pressures of the two scrolls and the intake manifold change with engine speed. It has an inherent vice that the large scroll pressure is higher than the intake pressure, resulting in reduced fuel economy.

(2) The asymmetric twin-scroll turbocharged engine with two EGR

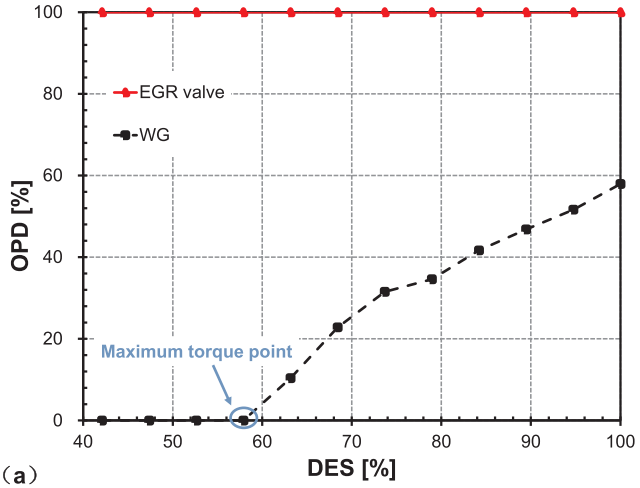

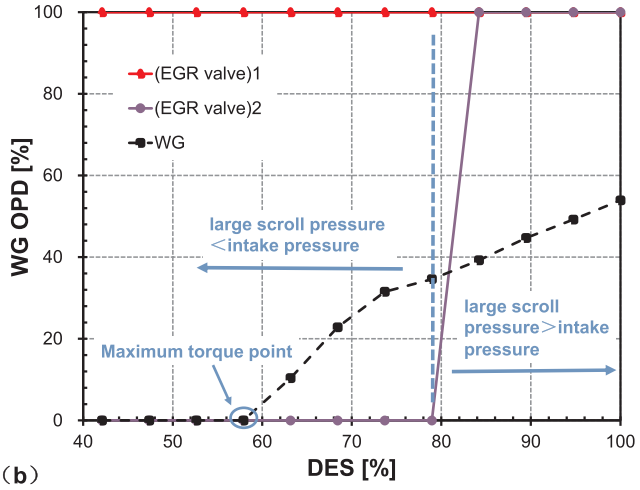

Fig. 18. For the maximum EGR rate, the OPDs relationship of the EGR valves and the WG in the (a) ATSTE-1EGR, and (b) ATSTE-2EGR.

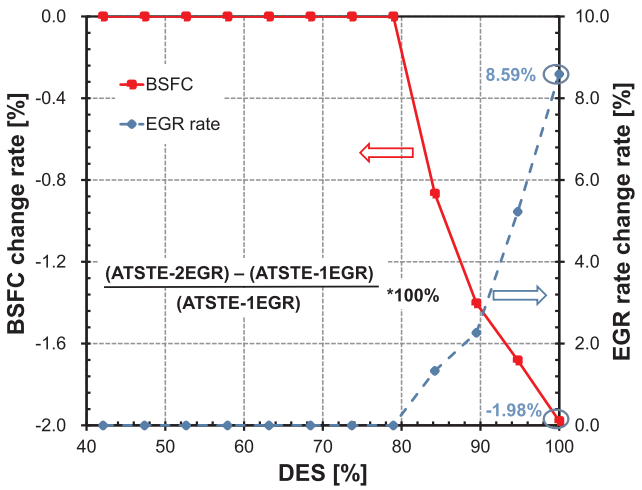

Fig. 19. Maximum EGR rate and BSFC improvements in the ATSTE-2EGR compared to the ATSTE-1EGR and expressed as a percentage of ATSTE-1EGR at 70% ASY versus different engine speeds.

circuits has a new control strategy of the two EGR valves and one wastegate. For the maximum EGR rate, The $(EGR\ valve)_1$ is fully open all the time and the $(EGR\ valve)_2$ is only open at high-speed range. Meanwhile, the wastegate will gradually open beyond the

maximum torque point for the engine boost-pressure limit.

(3) This study examined the influences of critical turbine parameters (asymmetry, efficiency and throat area). An increase in asymmetry results in an EGR rate increase and a BSFC decrease because the large scroll pressure is higher than the intake pressure for driving EGR and decreasing pumping loss. Changes in turbine efficiency and throat area have nearly identical effects, with performance improvements being observed with decreases in both turbine efficiency and throat area.

(4) The asymmetric twin-scroll turbocharged engine with two EGR circuits has better performances than that with one EGR circuit at the high-speed range. The improvements are zero and invariably before the $(\text{EGR valve})_2$ opens, and the maximum improvements EGR rate and BSFC are 8.59% and 1.98%, respectively.

The asymmetric twin-scroll turbocharged engine with two EGR circuits can effectively solve the problem of deteriorating fuel economy when the large scroll has a higher pressure than the intake. It is a new technical concept and approach for lower emissions and fuel consumption under more stringent legislations for internal combustion engines. This work may offer design principles for turbocharging and engine systems researchers. Different operations of the engine will be further studied and tested for better engine emissions and energy.

Acknowledgments

This research was supported by the National Natural Science Foundation of China (Grant No. 51876097).

References

[1] Wang S, Zhao F, Liu Z, Hao H. Heuristic method for automakers' technological strategy making towards fuel economy regulations based on genetic algorithm: a China's case under corporate average fuel consumption regulation. Appl Energy 2017;204:544–59.
[2] D'Ambrosio S, Ferrari A, Yan J. Diesel engines equipped with piezoelectric and solenoid injectors: hydraulic performance of the injectors and comparison of the emissions, noise and fuel consumption. Appl Energy 2018;211:1324–42.
[3] Jang SH, Choi JH. Comparison of fuel consumption and emission characteristics of various marine heavy fuel additives. Appl Energy 2016;179:36–44.
[4] Belgiornoa G, Dimitrakopoulosb N, Blasioa GD, Beatricea C, Tunestålb P, Tunérb M. Effect of the engine calibration parameters on gasoline partially premixed combustion performance and emissions compared to conventional diesel combustion in a light-duty Euro 6 engine. Appl Energy 2018;228:2221–34.
[5] Agarwal D, Singh SK, Agarwal AK. Effect of exhaust gas recirculation (EGR) on performance, emissions, deposits and durability of a constant speed compression ignition engine. Appl Energy 2011;88(8):2900–7.
[6] Raptotasios SI, Sakellaridis NF, Papagiannakis RG, Hountalas DT. Application of a multi-zone combustion model to investigate the NO_x reduction potential of two-stroke marine diesel engines using EGR. Appl Energy 2015;157:814–23.
[7] Almeida FL, Zoldak P, Wang Y, Sobiesiak A, Lacava PT. Multi-dimensional engine modeling study of EGR, fuel pressure, post-injection and compression ratio for a light duty diesel engine. In: Proceedings of the ASME 2014 internal combustion engine division fall technical conference; ICEF2014-5661.
[8] Zamboni G, Moggia S, Capobianco M. Hybrid EGR and turbocharging systems control for low NO_x and fuel consumption in an automotive diesel engine. Appl Energy 2016;165:839–48.
[9] Li W, Liu Z, Wang Z, Dou H. Experimental and theoretical analysis of effects of atomic, diatomic and polyatomic inert gases in air and EGR on mixture properties, combustion, thermal efficiency and NO_x emissions of a pilot-ignited NG engine. Energy Convers Manage 2015;105:1082–95.
[10] Wei H, Zhu T, Shu G, Tan L, Wang Y. Gasoline engine exhaust gas recirculation – a review. Appl Energy 2012;99(2):534–44.
[11] Saidur R, Rezaei M, Muzammil WK, Hassan MH, Paria S, Hasanuzzaman M. Technologies to recover exhaust heat from internal combustion engines. Renew Sustain Energy Rev 2012;16(8):5649–59.
[12] Hatami M, Cuijpers MCM, Boot MD. Experimental optimization of the vanes geometry for a variable geometry turbocharger (VGT) using a Design of Experiment (DoE) approach. Energy Convers Manage 2015;106:1057–70.
[13] Mao B, Yao M, Zheng Z, Liu H. Effects of dual loop EGR and variable geometry turbocharger on performance and emissions of a diesel engine. SAE technical paper 2016-01-2340. 2016.
[14] Furukawa H, Yamaguchi H, Takagi K, Okita A. Reliability on variable geometry turbine turbocharger. SAE technical paper 930194. 1993.
[15] Zhao R, Li W, Zhuge W, Zhang Y, Yin Y, Wu Y. Characterization of two-stage turbine system under steady and pulsating flow conditions. Energy 2018;148:407–23.
[16] Avola C, Copeland C, Burke R, Brace C. Effect of inter-stage phenomena on the performance prediction of two-stage turbocharging systems. Energy 2017;134:743–56.
[17] Zheng Z, Feng H, Mao B, Liu H, Yao M. A theoretical and experimental study on the effects of parameters of two-stage turbocharging system on performance of a heavy-duty diesel engine. Appl Therm Eng 2018;129:822–32.
[18] Westin F, Burenius R. Measurement of interstage losses of a two-stage turbocharger system in a turbocharger test rig. SAE technical paper 2010-01-1221. 2010.
[19] Feneley AJ, Pesiridis A, Andwari AM. Variable geometry turbocharger technologies for exhaust energy recovery and boosting-a review. Renew Sustain Energy Rev 2016;71:959–75.
[20] Schorn NA. The radial turbine for small turbocharger applications: evolution and analytical methods for twin-entry turbine turbochargers. SAE Int J Engines 2014;27(3):1422–42.
[21] Chiong MS, Rajoo S, Romagnoli A, Costall AW, Martinez-Botas RF. One-dimensional pulse-flow modeling of a twin-scroll turbine. Energy 2016;115:1291–304.
[22] Rajoo S, Romagnoli A, Martinez-Botas RF. Unsteady performance analysis of a twin-entry variable geometry turbocharger turbine. Energy 2012;38(1):176–89.
[23] Chiong MS, Rajoo S, Martinez-Botas RF, Costall AW. Engine turbocharger performance prediction: one-dimensional modeling of a twin entry turbine. Energy Convers Manage 2012;57(2):68–78.
[24] Baert RS, Beckman DE, Veen A. Efficient EGR technology for future HD diesel engine emission targets. SAE technical paper 1999-01-0837. 1999.
[25] Müller M, Streule T, Sumser S, Hertweck G, Nolte A, Schmid W. The asymmetric twin scroll turbine for exhaust gas turbochargers. In: Proceedings of the ASME turbo expo 2008: power for land, sea and air; 2008. Paper GT2008-50614.
[26] Fredriksson CF, Qiu X, Baines NC, Müller M, Brinkert N, Gutmann C. Meanline modeling of radial inflow turbine with twin-entry scroll. In: Proceedings of the ASME turbo expo 2012: turbine technical conference and exposition; 2012. Paper GT 2012-69018.
[27] Krüger W, Kleffel J, Dietrich P, Koch D. 10.7-l Daimler HD truck engine for Euro VI and Tier 4. MTZ Worldwide 2012;73(12):4–10.
[28] Hoffmann K, Benz M, Weirich M, Herrmann HO. The new Mercedes-Benz medium duty commercial natural gas engine. MTZ Worldwide 2014;75(11):4–11.
[29] Herrmann HO, Kožuch P, Lettmann H, Brünemann R. The latest heavy-duty engine generation from Mercedes-Benz Part 2: combustion and emissions. MTZ Worldwide 2016;77(7–8):58–63.
[30] Burny BD. New 14.8-l HD truck engine from Daimler for NAFTA. MTZ Worldwide 2013;74(12):12–9.
[31] Hand MJ, Hellström E, Kim D, Stefanopoulou A, Kollien J, Savonen C. Model and calibration of a diesel engine air path with an asymmetric twin scroll turbine. In: Proceedings of the ASME internal combustion engine division fall technical conference; 2013. Paper ICEF2013-19134.
[32] Brinkert N, Sumser S, Weber S, Fieweger K, Schulz A, Bauer HJ. Understanding the twin scroll turbine: flow similarity. J Turbomachinery 2013;135(2):021039.
[33] Zhu D, Zheng X. Asymmetric twin-scroll turbocharging in diesel engines for energy and emission improvement. Energy 2017;141:702–14.
[34] Zhu D, Zheng X. A new asymmetric twin-scroll turbine with two wastegates for energy improvements in diesel engines. Appl Energy 2018;233:263–72.
[35] Schmidt S, Rose MG, Müller M, Sumser S, Chebli E, Streule T, Stiller M, Leweux J. Variable asymmetric turbine for heavy duty truck engines. In: Proceedings of the ASME turbo expo 2013: turbine technical conference and exposition; 2013. Paper GT2013-94590.
[36] Heywood JB. Internal combustion engine fundamentals. McGraw-Hill; 1988.
[37] Uhlmann T, Lückmann D, Aymanns R, Scharf J, Höpke B, Scassa M, et al. Development and matching of double entry turbines for the next generation of highly boosted gasoline engines. XXII Simpósio Internacional de Engenharia Automotiva. 2014. p. 777–814.
[38] Zamboni G, Capobianco M. Experimental study on the effects of HP and LP EGR in an automotive turbocharged diesel engine. Appl Energy 2012;94(2):117–28.